

Resonant Electromagnetic Vibration Harvesters feeding Sensor Nodes for real-time Diagnostics and Monitoring in Railway Vehicles for Goods Transportation: a numerical-experimental analysis

Oswaldo Brignole, Claudio Cavalletti,
Antonino Maresca, Nadia Mazzino
Ansaldo STS
Genova, Italy

Marco Balato, Antonio Buonomo, Luigi Costanzo,
Massimiliano Giorgio, Roberto Langella, Alessandro
Lo Schiavo, Alfredo Testa, Massimo Vitelli
Department of Industrial and Information Engineering
Second University of Naples
Aversa (CE), Italy

Abstract—In this paper, the results of a combined numerical-experimental analysis on a system, part of a wireless sensor network, composed by a resonant electromagnetic energy harvester, a suitable power electronic interface and a sensor node are presented and discussed. Such a system is to be used onboard for real-time diagnostics and monitoring in railway vehicles for goods transportation.

Keywords—*diagnostic, energy harvesting, rail vehicles, safety.*

I. INTRODUCTION

In order to increase the safety of railways transport systems and to reduce the maintenance costs it is necessary to develop and optimize suitable low-cost monitoring and diagnostic systems [1]-[3]. This is one of the aims of the MODISTA project which is devoted just to the study, development and optimization of innovative technological and methodological solutions. In particular, one of the Work-Packages of the above project is represented by the “Application of Green Technologies” with specific reference, among the others, to vibration energy harvesters. In this paper we will focus the attention on Resonant Electromagnetic Vibration Energy Harvesters (REVEHs) [4]-[9]. In particular, the possibility to generate directly onboard, by means of suitable REVEHs, the electric power needed to supply the sensor nodes of the monitoring and diagnostic system will be explored. It will be shown that: 1) the commercial REVEHs which are available at the moment on the market [10]-[11] are not suitable at all for the considered application; 2) the theoretical studies which have been reported in the literature with specific reference to sinusoidal vibrations are not enough to analyze those practical applications (like the one considered in this paper) which are instead characterized by the occurrence of non sinusoidal vibrations; 3) the need exists to develop smart power electronics interfaces which are able to allow the maximum power extraction from the REVEHs in any operating condition.

II. AUTONOMOUS MONITORING AND DIAGNOSTIC SYSTEM

In order to monitor the vehicle health conditions, to prevent accidents and to improve the safety in presence of potentially dangerous goods, it is necessary to design a control platform

composed of an onboard and a wayside system. In this paper we will focus the attention on the onboard system. In particular we will analyze the possibility to generate directly onboard, by means of suitable REVEHs, the electric power needed to supply the sensor nodes of the onboard system. In fact, on freight wagons, an on board power supply is not available. The onboard system will be composed by (see Fig. 1):

- A number of sensor nodes.
- A control unit for the acquisition of the data collected by the onboard sensor units and for their subsequent pre-processing with the aim of obtaining aggregate data to be used by the wayside control center.
- A wireless communication module (eg. GSM) to send such data to the control center.
- A geolocation module (GPS) which could be used for traceability purposes of the freight wagon, for the monitoring of its dwell times and for the checking of the train integrity.
- An autonomous power supply system composed by energy-harvesting and energy storage systems which must be sized on the basis of the energy requirements of the sensor nodes and of the characteristics of the vibrations in the installation points of the harvesters.

III. PRELIMINAR EXPERIMENTAL ACTIVITY

In order to explore the possibility to feed a sensor node by means of a suitable REVEH, it is preliminarily necessary to know both the vibration characteristics (that is amplitudes, dominant frequencies, dependence on the time varying speed of the freight wagons) and the load characteristics (that is its operating voltage which is usually constant, and the time domain profile of its operating current).

III.1 VIBRATION CHARACTERISTICS

The freight wagon which has been used in the experimental activity is equipped with Y25 bogies, which currently are the most diffused in Europe for this kind of vehicles. A number of train rides have been performed on a path whose length is 25 km. Different speeds and two different operating conditions (no load and heavy load) have been adopted. The detailed

description of the whole set of rides and of the corresponding freight train speed profiles versus the traveled distance can be found in [12].

The accelerometers which have been used to record the vibration signals are Slam Stick X - LOG-0002 produced by Mide [13]. The main characteristics of the data logger are: Sampling Rate: 100 Hz to 20 kHz; Tunable Anti Aliasing filter; Acceleration Ranges: ± 25 g, ± 100 g, & ± 500 g; Storage Size: 2GB; Size (in): 3 x 1.18 x 0.59; Mass: 40 & 65 grams; Sensors: Triaxial Accelerometer, Temperature, Pressure. The sampling frequency has been set to 20 kHz and the anti aliasing filter frequency has been set to 4 kHz. The accelerations along 3 axes: X, Y (horizontal axes) and Z (vertical axis) have been recorded. Accelerometers have been installed in different positions of the freight train as shown in Fig. 2. As an example, in Figs. 3 and 4 two accelerations signals which have been recorded in position A1 (Fig.2), along the Z axis, are reported. The duration of both signals is 25 s. In

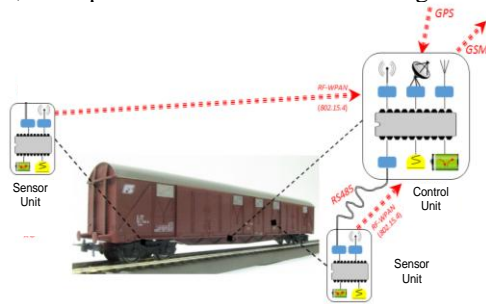


Fig. 1. Autonomous Monitoring and Diagnostic System.

particular, the signal which is shown in Fig. 3 (Fig. 4) has been obtained in correspondence of a nearly constant speed of the freight wagon equal to about 75 km/h (95 km/h).

The main results of the experimental campaign are the following ones:

- as expected, the maximum accelerations have been registered along the Z axis;
- the higher the train speed the higher the acceleration amplitudes;
- the maximum of the vibrations energy is concentrated around 867 Hz with a broad band behavior;
- the presence of a quite heavy load doesn't change the frequency positions of the main tones but their amplitude is amplified in the range centered around 867 Hz where their amplitude is maximum;
- positions A1 and E1 are characterized by the maximum amplitudes.

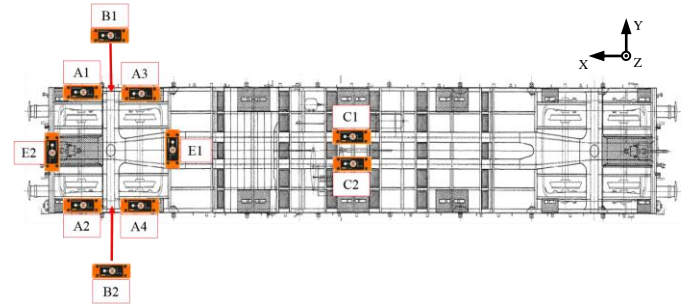


Fig. 2. Accelerometers positions.

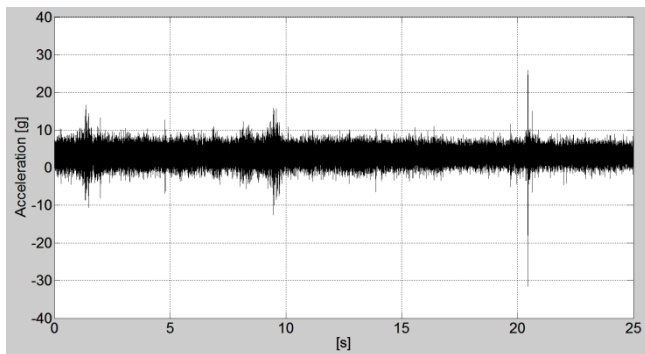


Fig. 3. Acceleration signal in position A1, along the Z axis, in correspondence of a nearly constant speed of the freight wagon equal to about 75 km/h.

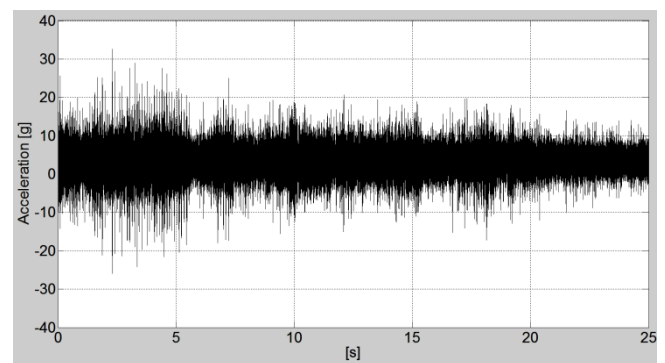


Fig. 4. Acceleration signal in position A1, along the Z axis, in correspondence of a nearly constant speed of the freight wagon equal to about 95 km/h.

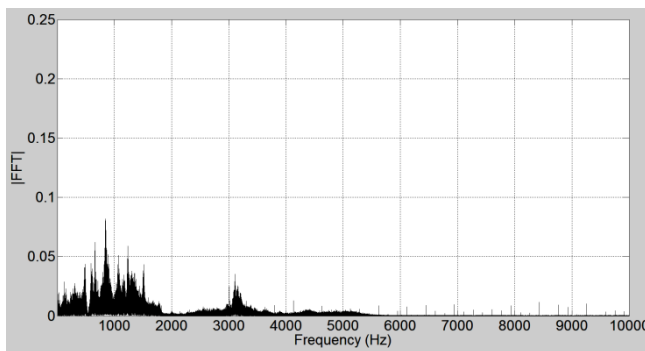


Fig. 5. Magnitude of the FFT of the signal of Fig. 3.

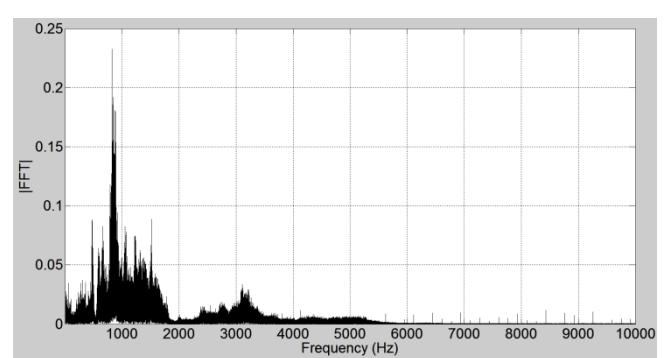


Fig. 6. Magnitude of the FFT of the signal of Fig. 4.

We explicitly remark here that, to the best of the authors' knowledge, in the literature very few documents only contain data on vibrations onboard freight wagons. In most cases such data refer to international norms (such as the UNI EN 13848-

5, ENR B176) which are specifically devoted to the identification of the geometric quality of railway lines and that consider low-frequency (up to 15-20 Hz) vibrations [14]-[16]. In [17], which instead refers to the only commercial product

IV. REVEH AND POWER ELECTRONICS INTERFACE CHARACTERISTICS

As evidenced before, the resonant frequencies of the commercially available REVEHs [10]-[11] are much lower than the dominant frequencies of the vibration signals which have been recorded on the freight wagon and used for the experimental activity. Therefore, the commercial REVEHs which are available at the moment on the market need proper modifications in order to become suitable for the considered application. Indeed, as explained in the following sub-sections, also the commercial power electronics device to be used between the source (the REVEH) and the load (the sensor node) requires a proper tuning in order to optimize the overall performances of the whole system.

IV.1 REVEH CHARACTERISTICS

The equivalent electric circuit of a REVEH is shown in Fig. 10 [6], [8]. L_c is the coil inductance, R_c is the coil resistance, $\ddot{z}(t)=A_{MAX}\cdot\cos(\omega t)$ is the base acceleration with an angular frequency ω . Moreover, the values of the resistance R_m , of the inductance L_m and of the capacitance C_m depend on the electromechanical parameters of the harvester: $R_m=\theta^2/c$ (c is the viscous damping coefficient and θ is the electromechanical coupling coefficient), $L_m=\theta^2/k_s$ (k_s is the stiffness coefficient), $C_m=m/\theta^2$ (m is the vibrating mass).

In what follows, the commercial electromagnetic vibration energy harvester PMG17-100 by Perpetuum [10] will be considered. The main characteristics of the PMG17-100 harvester are: $R_c=3800\ \Omega$; $L_c=3.9\ \text{H}$; $R_m=347\ \Omega$; $L_m=0.0864\ \text{H}$; $C_m=29.33\ \text{mF}$, $m/\theta=0.0015\ \text{kg}\cdot\text{m}/(\text{V}\cdot\text{s})$ [24]. Indeed, since the resonant frequency of the PMG17-100 is equal to 100 Hz and, therefore, it is not suitable for the considered application, we have considered a virtual REVEH (identified in the following text as VREVEH) which has exactly the same shape of the Power vs. frequency characteristic of the PMG17-100 but with a different resonant frequency. In particular, the resonant frequency of the VREVEH is just equal to 867 Hz and its 50% power bandwidth is 17Hz. The Power vs. frequency characteristic at $A_{MAX}=1\ \text{g}_{RMS}$ of the VREVEH is shown in Fig. 11. The main characteristics of the VREVEH harvester are: $R_c=3800\ \Omega$; $L_c=3.9\ \text{H}$; $R_m=3800\ \Omega$; $L_m=0.0096\ \text{H}$; $C_m=3.5\ \text{mF}$ [24]. It is worth noting that, although the VREVEH is perfectly tuned with the vibrations taking place in the considered application, and, although it seems to be able to provide enough power (50 mW at 1 g_{RMS}), if the power electronics interface does not properly work, the VREVEH is not enough to feed the considered sensor node. Such an aspect will be discussed in Section V.

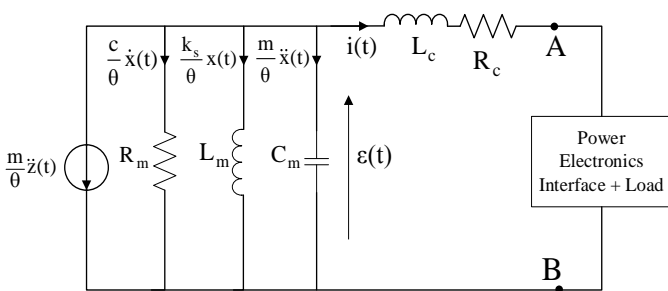


Fig. 10. Equivalent electric circuit of a REVEH feeding a load.

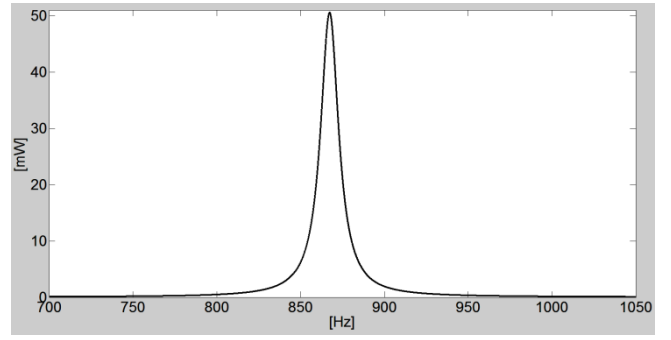


Fig. 11: Power vs. frequency characteristic of the VREVEH.

IV.2 POWER ELECTRONICS INTERFACE CHARACTERISTICS

The power electronics device that has been considered for the simulations which are discussed in Section V is the Linear Technology chip LTC3331 [25]. It allows the management of both a REVEH and a battery by means of the combined use of two switching regulators: a buck and a buck-boost. Such converters are controlled by a prioritizer that selects which converter to use on the base of the availability of energy from the battery and/or from the harvester. If harvested energy is available, the buck regulator is active and the buck-boost is off. If instead harvested energy is not available, the buck regulator is off and the buck-boost is active feeding the load with battery energy. The LTC3331 block diagram together with all the electrical components which are necessary for its proper operation are shown in Fig. 12.

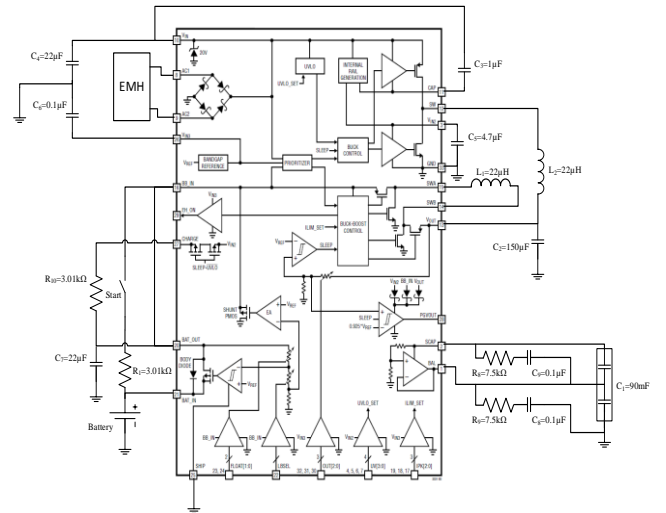


Fig. 12. LTC3331 block diagram with the electrical components adopted for numerical simulations.

An internal full-wave bridge rectifier, accessible via the AC1 and AC2 inputs, rectifies AC sources such as the VREVEH. The capacitor C_4 at the VIN pin is used as an energy reservoir for the buck converter. The bridge rectifier has a total drop of about 800 mV and is capable of carrying up to 50 mA. When the voltage across C_4 rises above the rising threshold (UVLOR), the buck converter is enabled and charge is transferred from C_4 to the output capacitor C_2 . When the voltage across C_4 is depleted below the falling threshold (UVLOF), the buck converter is disabled. These thresholds can be set from 4V to 18V (with large or small hysteresis windows) through the UV0-UV3 pins [25]. The buck regulator uses a hysteretic voltage algorithm to control the output voltage V_{out} through internal feedback from the V_{out} sense

pin. When the buck brings V_{out} into regulation, the buck itself enters a low quiescent current sleep state that monitors the output voltage with a sleep comparator. During this operating mode, load current is provided by the buck output capacitor C_2 . When the output voltage falls below the regulation point, the buck regulator wakes up and the cycle repeats. This hysteretic method of providing a regulated output reduces switching losses. V_{out} can be set from 1.8V to 5.0V via the output voltage select bits OUT0-OUT2 [25]. The buck-boost uses the same hysteretic algorithm as the buck to control V_{out} , with the same sleep comparator. The buck-boost has three modes of operation: buck, buck-boost and boost. An internal mode comparator determines the mode of operation based on the values of the battery voltage and of V_{out} . An integrated battery charger charges the battery through the BB_IN pin. Connecting BB_IN to the BAT_OUT pin, an internal MOSFET switch will then connect the battery charger to BAT_IN. The battery charger is a shunt regulator which can sink up to 10mA. The battery float voltage is programmable with two bits and a third bit is used to program the battery connect and disconnect voltage levels. This disconnect feature protects the battery from permanent damage by deep discharge.

V. NUMERICAL RESULTS

In Fig 13 a screen shoot of the LTSPICE simulator [26] implementing the LTC3331 fed by the VREVEH is shown. The sensor node is simulated by means of a current generator (I_{load}) which is characterised by the same current which is drawn by the sensor node (see Fig. 9); $I_{acc} = \ddot{z}(t) \cdot m / \theta$. In Fig. 14 such a current is shown in the case $T^* = 20$ s.

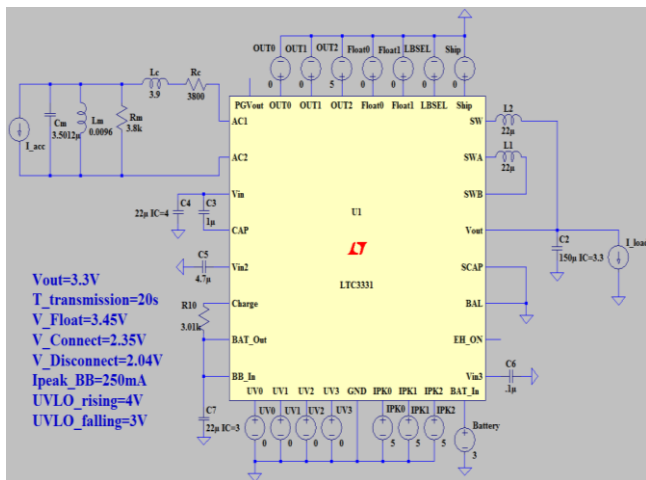


Fig. 13. Screen shoot of the LTSPICE simulator implementing the LTC3331 fed by a Resonant Electromagnetic Harvester.

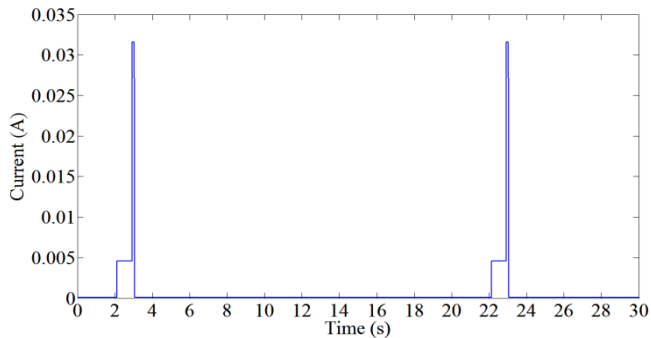


Fig. 14. Current of the generator representing the sensor node, $T^* = 20$ s.

The numerical results which are presented in this Section have been obtained by using the acceleration signal which is shown in Fig. 3 (freight wagon speed=75 km/h). They are summarized in Tab. 2.

The meaning of the symbols of Tab. 2 is the following one. R_{Vin} is the Range of V_{in} and it has been set by means of the UV0-UV3 pins [25].

V_{AV} is the Average value of V_{in} ; due to the hysteretic control of V_{in} , V_{AV} does not necessarily fall inside the selected R_{Vin} since, the UVLOR can be exceeded by V_{in} while V_{in} cannot drop below the UVLOF.

P_{Load} is the average Load power; of course the higher T^* the lower P_{Load} .

DP is the difference between the average harvested power and P_{Load} . When DP is > 0 the VREVEH is able to feed the sensor node and to charge the battery at the same time; when DP is < 0 the VREVEH is not able to feed the sensor node without the help of the battery.

E_{APH} is the Average Percent Harvested Energy: $E_{APH} = 100 \cdot (P_{Load} + DP) / (P_{Load})$. Of course, values of E_{APH} greater than 100 indicate that the VREVEH is able to feed the sensor node and to charge the battery at the same time; instead, values of E_{APH} lower than 100 indicate that the VREVEH is not able to feed the sensor node without the help of the battery.

By analyzing the data reported in Tab. 2 it is clearly evident that the selected R_{Vin} (and the resulting value of V_{AV}) plays a very strong role.

In particular, in the case $T^* = 20$ s, a unique value of R_{Vin} ($R_{Vin} = 4V - 3V$) is able to lead to $DP > 0$ while in the case $T^* = 30$ s the last five possible settings are able to successfully supply the load. In the case $T^* = 60$ s, with the only exception of the first setting point ($R_{Vin} = 18V - 17V$), the VREVEH is always able to feed the sensor node.

Finally, it is worthwhile noting that setting the R_{Vin} in the range 04V-03V allows successfully supplying the sensor node for the speed considered and for all of the analyzed duty-cycles (T^*).

Of course, when the speed varies different results can be obtained so demonstrating that the identification of the optimal R_{Vin} is of the utmost importance.

Table 2: R_{Vin} , V_{AV} , ΔP , P_{Load} , P_{APH} and T^* for different LTSpice simulations

T^* [s]	R_{Vin} [V]	V_{AV} [V]	P_{Load} [mW]	DP [mW]	E_{APH} %
20	18-17	17.6	1.6	-1.2	23
20	18-05	12.7	1.6	0	44
20	16-15	15.7	1.6	-0.01	32
20	16-05	11.5	1.6	-0.72	55
20	14-13	14.0	1.6	-0.96	40
20	14-05	10.3	1.6	-0.63	61
20	12-11	12.1	1.6	-0.81	49
20	12-05	9.3	1.6	-5.52	65
20	10-09	10.4	1.6	-0.65	59
20	10-05	8.7	1.6	-0.48	70
20	08-05	7.7	1.6	-0.43	73
20	08-07	8.6	1.6	-0.42	74
20	07-06	7.5	1.6	-0.42	74
20	06-05	6.9	1.6	-0.36	77
20	05-04	6.0	1.6	-0.3	81
20	04-03	6.1	1.6	1.1	169
30	18-17	17.7	1.145	-0.73	36
30	18-05	12.7	1.145	0	69
30	16-15	15.8	1.145	-0.6	48
30	16-05	11.7	1.145	-0.27	76
30	14-13	14.1	1.145	-0.47	59
30	14-05	10.7	1.145	-0.2	83
30	12-11	12.3	1.145	-0.34	71

30	12-05	9.6	1.145	-0.08	93
30	10-09	10.6	1.145	-0.18	84
30	10-05	8.9	1.145	-0.03	97
30	08-07	8.9	1.145	-0.03	97
30	08-05	8.1	1.145	0.03	103
30	07-06	8.0	1.145	0.04	103
30	06-05	7.2	1.145	0.1	109
30	05-04	6.4	1.145	0.17	114
30	04-03	6.3	1.145	1.1	198
60	18-17	17.7	0.68	-0.12	83
60	18-05	12.5	0.68	0.38	156
60	16-15	15.9	0.68	0.02	102
60	16-05	11.8	0.68	0.35	151
60	14-13	14.2	0.68	0.14	121
60	14-05	10.9	0.68	0.42	162
60	12-11	12.5	0.68	0.27	140
60	12-05	9.9	0.68	0.5	174
60	10-09	10.8	0.68	0.43	162
60	10-05	9.2	0.68	0.56	182
60	08-05	8.5	0.68	0.63	192
60	08-07	9.2	0.68	0.56	183
60	07-06	8.5	0.68	0.63	192
60	06-05	7.7	0.68	0.69	201
60	05-04	7.0	0.68	0.7	210
60	04-03	6.8	0.68	1.2	282

Moreover, since the speed of the train changes with time, also the characteristics of the associated vibrations change. As a consequence, the optimal value of R_{vin} may change with time. We explicitly remark here that, to the best of the authors' knowledge, no theoretical guideline is available in the literature on such an aspect. Moreover, since in the literature nearly always only sinusoidal vibrations are considered, the need exists for further investigations on systems which are characterized by the presence of non sinusoidal vibrations. The aim of such investigations is the identification of suitable guidelines for the development of smart electronic interfaces which are able to track the time-varying maximum power operating point of the REVEHs in arbitrary operating conditions.

VI. CONCLUSIONS

The results of a numerical-experimental analysis on a system, part of a Wireless Sensor Network, composed by a REVEH, a power electronics interface and a Sensor Node to be used for real-time diagnostics and monitoring in railway vehicles for goods transportation has been presented and discussed. The main conclusions are the following ones. The commercial REVEHs which are available at the moment on the market are characterized by resonant frequencies which are too low for the considered application. For this reason, a virtual REVEH which has exactly the same Power vs. frequency characteristic of the only commercial available REVEH but with a different resonant frequency has been considered. In particular, it was demonstrated that the set of the input voltage range of the electronic interface between the harvester and the electronic load plays a crucial role in the design of the system. Further investigations are needed with specific reference to systems which are characterized by non sinusoidal vibrations. The need exists to develop smart power electronics interfaces with auto-tuning capabilities in order to allow the maximum power extraction from the REVEHs in arbitrary operating conditions.

ACKNOWLEDGMENT

This research activity is supported by the Italian Ministero dell'Istruzione, dell'Università e della Ricerca (MIUR) in the frame of MODISTA project.

REFERENCES

- [1] Fraunhofer LBF, "Enhanced safety for rail transport". S. M. Rakshit, M. Hempel, H. Sharif, J. Punwani, M. Stewart, S. Mehrvarzi, "Challenges in current wireless sensor technology for railcar status monitoring for North America's freight railroad industry", 2012 Joint Rail Conference, pp.397-405, 2012, American Society of Mechanical Engineers.
- [2] T. Lin, W. John, Z. Lei, "Energy Harvesting from Rail Track for Transportation Safety and Monitoring", National Technical Information Service 2014.
- [3] C.B. Williams, R.B. Yates: "Analysis of a micro-electric generator for microsystems", Sensors and Actuators A: Physical, Elsevier, 1996, Num 52, pp. 8-11.
- [4] Glynne-Jones, P., Tudor, M. J., Beeby, S. P., & White, N. M. (2004). "An electromagnetic, vibration-powered generator for intelligent sensor systems". Sensors and Actuators A: Physical, 110(1), 344-349.
- [5] Khaligh, A.; Peng Zeng; Cong Zheng, "Kinetic Energy Harvesting Using Piezoelectric and Electromagnetic Technologies—State of the Art", in Industrial Electronics, IEEE Transactions on , vol.57, no.3, pp.850-860, March 2010, doi: 10.1109/TIE.2009.2024652.
- [6] D. Zhu, S. Roberts, T. Mouille, M.J Tudor, S.P Beeby: "General model with experimental validation of electrical resonant frequency tuning of electromagnetic vibration energy harvesters", SMART MATERIALS AND STRUCTURES, 2012, Num 21, pp. 1-14, doi:10.1088/0964-1726/21/10/105039.
- [7] D Zhua, S. Roberts, M.J. Tudor, S.P. Beeby: "Design and experimental characterization of a tunable vibration-based electromagnetic micro-generator", Elsevier, Sensors and Actuators A: Physical, Num 158, 2010, pp. 284–293, doi:10.1016/j.sna.2010.01.002.
- [8] N.G. Elvin, A.A. Elvin: "An experimentally validated electromagnetic energy harvester", Elsevier, Journal of Sound and Vibration, 2011, Num 330, pp. 2314–2324, doi:10.1016/j.jsv.2010.11.024.
- [9] P.D. Mitcheson, T.T. Toh, K. H. Wong, S.G. Burrow, A.S. Holmes, "Tuning the Resonant Frequency and Damping of an Electromagnetic Energy Harvester Using Power Electronics", IEEE Transactions on Circuits and Systems II: Express Briefs, vol.58, no.12, Dec. 2011.
- [10] <http://www.perpetuum.com>
- [11] <http://www.ferrosi.com>
- [12] O. Brignole, C. Cavalletti, G. Lauro, A. Maresca, N. Mazzino, M. Balato, A. Buonomo, L. Costanzo, M. Giorgio, R. Langella, A. Lo Schiavo, D. Scaldarella, A. Testa, L. Verde, M. Vitelli: "Real-time Diagnostic and Monitoring on Railway Vehicles for Goods Transportation", CONVEGNO ANNUALE INTERNAZIONALE AEIT, Napoli, 14-16 ottobre 2015, pp. .
- [13] <http://www.mide.com/pdfs/slam-stick-x-datasheet.pdf>.
- [14] G.De Pasquale, N. Zampieri, "Progettazione di generatori elettromeccanici con recupero di energia cinetica vibrazionale a bordo di treni merci", 40° Convegno Nazionale AIAS, Palermo, 2011.
- [15] A. Bracciali, L. Di Benedetto, F. Piccioli, "ANALISI STATISTICA DELLE VIBRAZIONI MISURATE SULLE BOCCOLE DELLE SALE FERROVIARIE", 40° Convegno Nazionale AIAS, Palermo, 2011.
- [16] P. Shahidi, D. Maraini, B. Hopkins, A. Seidel, " Estimation of Bogie Performance Criteria Through On-Board Condition Monitoring", ANNUAL CONFERENCE OF THE PROGNOSTICS AND HEALTH MANAGEMENT SOCIETY 2014, pp. 1-10.
- [17] <http://www.perpetuum.com/pmgrail.asp>
- [18] <http://realvibrations.niplab.org/search/node/train>
- [19] <http://ww1.microchip.com/downloads/en/DeviceDoc/39932D.pdf>
- [20] <http://ww1.microchip.com/downloads/en/DeviceDoc/70329b.pdf>
- [21] <http://www.ti.com/lit/ds/symlink/lm60.pdf>
- [22] <http://www.analog.com/media/en/technical-documentation/data-sheets/ADXL363.pdf>
- [23] <https://www.bourns.com/pdfs/90SERS.pdf>
- [24] M. Balato, L. Costanzo, M. Vitelli, "Identification of the parameters of the equivalent electric circuit of electromagnetic harvesters", 4th International Conference on Renewable Energy Research and Applications, ICRERA 2015, Palermo, 22-25 Nov. 2015, pp. .
- [25] <http://cde.linear.com/docs/en/datasheet/3331fc.pdf>
- [26] <http://www.linear.com/designtools/software/>